Late Miocene "washhouse" climate in Europe

Madelaine Böhme [a,*], August Ilg [b], Michael Winklhofer [a]

[a] Geo-Bio-Centre[LMU], Department of Earth- and Environmental Science, Ludwig-Maximillians University, Munich 80333, Germany
[b] Schumannstrasse 83, Düsseldorf 40237, Germany

ARTICLE INFO

ABSTRACT

We present two eight-million year long proxy records of precipitation for Southwest and Central Europe, covering the middle to late Miocene (5.3–13 Ma) at a temporal resolution of about 60 kyr and 150 kyr, respectively. The estimates of precipitation are based on the ecophysiological structure of herpetological assemblages (amphibians and reptiles). From 13.0 Ma until about 9 Ma, both records show a similar trend, evolving from a long dry period (13–11 Ma) into a "washhouse climate" (10.2–9.8 Ma), characterized by global warm conditions and several times more precipitation than present. The transition from washhouse to a dryer climate between 9.7 and 9.5 Ma and the concomitant cooling episode appear to have triggered a severe biotic event known as the Vallesian crisis, which included the extinction of hominoids in Western Europe. A second washhouse period (9.0–8.5 Ma), coeval with a global warm episode, was unprecedentedly intense in Southwest Europe, but less pronounced in Central Europe. From 8 Ma onward, a divergence in the two precipitation records is observed, with Southwest Europe staying wetter and Central Europe becoming dryer than present. Both precipitation records are combined into a common run-off curve as a measure of the relative intensity of the hydrological cycle for moderate latitudes of continental Europe. The run-off curve shows a remarkable positive correlation with Atlantic deep-water temperatures from Ceará Rise by Lear et al. (2003), which are significantly higher (up to +3 °C) during the two washhouse periods and show no other positive excursion of comparable magnitude. We discuss potential links and the role of the coeval temporary restriction of the Central American Seaway on ocean and atmosphere circulation.

© 2008 Elsevier B.V. All rights reserved.

1. Introduction

The late Miocene has attracted recent interest as a potential model system for testing future climate change scenarios (Lunt et al., 2008a). Model predictions for future global warming (IPPC, 2007) project an increase in global mean precipitation with substantial spatial variations, e.g. between northern Europe (wetter than present) and southern Europe (drier than present). Climate proxy data for the Tortonian (11.6–7 Ma) indicate warmer and more humid conditions than today in continental Europe (e.g., Mosbrugger et al., 2005; Bruch et al., 2006), an already well-developed Antarctic ice cap, and a mostly ice-free Greenland (Thiede et al., 1998). The land–sea distribution was similar to present, but probably with less pronounced topography and still open oceanic gateways that now are either completely closed (Isthmus of Panama) or at least restricted for large-scale oceanic interexchange (Indonesian seaway). Overall warmer ocean temperatures have been deduced from deep-sea proxy records (Zachos et al., 2001; Lear et al., 2003). For such a scenario, it is reasonable to expect higher sea-surface temperatures in the North Atlantic and an enhanced northward heat transport and moisture supply from low to high latitudes, leading to an intensified hydrological cycle in

Europe. This is also suggested by a paleoprecipitation map for Europe reconstructed from paleoflora analysis (Fig. 6 in Bruch et al., 2006). Because of the less accurate dating of many palaeobotanical sites such maps typically contain data with low temporal resolution (in this case from 11–7 Ma). However, the late middle and late Miocene are characterized by several cooling and warming events (Mudie and Helgason, 1983; Thiede et al., 1998; Winkler et al., 2002; Billups and Schrag, 2002), which underline the need for higher temporal resolution of palaeoprecipitation data.

To learn more about the long-term variations of the hydrological cycle in the late middle and late Miocene, we have constructed two eight-million year long paleoprecipitation proxy records for two European regions, with characteristic time resolution of ~100 kyr. The stratigraphic–chronologic framework is provided by cyclostratigraphic, magnetostratigraphic and/or small mammal based biostratigraphic methods. A precipitation database was established using the ecophysiological structure of herpetological (amphibians and reptiles) assemblages (Böhme et al., 2006) stemming from two regions in the European sector of the North Atlantic catchment area (Fig. 1): the Calatayud–Teruel Basin in Southwest Europe (13.56 to 5.36 Ma) and the Parathethys region in Central–Eastern Europe (13.27 to 5.75 Ma). The median temporal resolution of each record is ~60 kyr and ~150 kyr, respectively. Since the regions investigated have a different spatial extent, we will later express the precipitation in terms of an
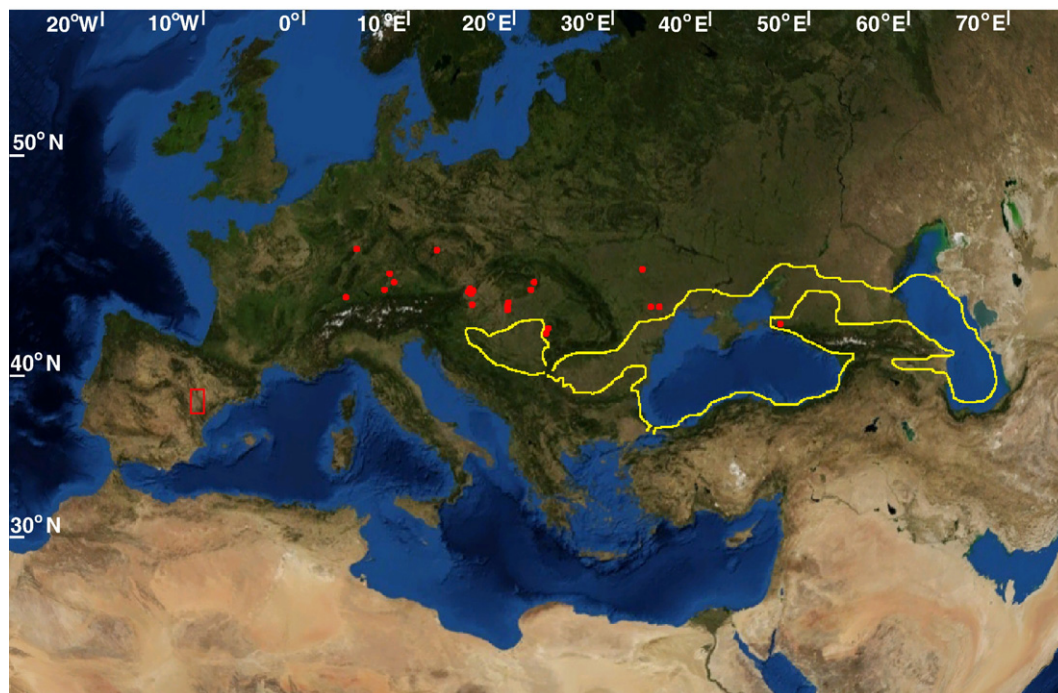
Fig. 1. Map of western Eurasia showing the coastline (yellow) of the Central and Eastern Paratethys Sea around 8 Ma, according to Popov et al., 2004, 2006), the position of localities used for reconstructing the Central and Eastern European precipitation curve (red dots), and the South-West European precipitation curve (red rectangular; Calatayud–Teruel Basin).

area-weighted continental run-off as an indicator of the intensity of the hydrological cycle.

2. Methods

2.1. Stratigraphic–chronological framework

2.1.1. Southwest Europe

The fossil record of amphibian and reptilian communities comes from two continental sequences of NE Spain (Calatayud–Daroca and Teruel Basin), both representing endorheic basins. Fossils were found in alluvial and lacustrine facies of the basin margins which may laterally grade into evaporites.

18 fossil-bearing horizons from the Calatayud–Daroca Basin were sampled from an area of few square kilometres east of the Villafeliche village, (see Fig. 2 in Daams et al., 1999). The composite section comprises over 200 m sediments of alluvial and lacustrine origin.

52 fossil-bearing horizons from the Teruel Basin were sampled from an area of up to 100 km^2 between the Teruel and Alfambra villages (Van Dam et al., 2001) and south of Teruel (Abdul Aziz et al., 2004). The composite section comprises over 200 m sediments of alluvial and lacustrine origin.

The age model for the 70 horizons (localities) is according to the one established by Van Dam et al. (2006), which is based on correlation to local magnetostratigraphically dated sections, cyclo- and lithostratigraphic extrapolation, and biostratigraphic correlation. For details see Van Dam et al. (2006). The fossil amphibians and reptiles we used for the estimation of paleoprecipitation were picked out from exactly the same sediment samples from which Van Dam et al. (2006) derived their small mammal record.

2.1.2. Central- and Eastern Europe

The fossil record of amphibian and reptilian communities was obtained from several locations of the Paratethys region (Western Paratethys: North Alpine Foreland Basin, Central Paratethys: Vienna, Pannonian, Transylvanian Basins, Eastern Paratethys region, see Fig. 1 for sampling sites). The sites contributing to the Paratethys precipitation record range from 46.5°N to 49.5°N in latitude and 8°E (Switzerland) to 28°E (Moldova) in longitude; a single locality is from 40°E (Southern Russia). Combining data from such a wide geographic band may appear difficult because of possible regional precipitation gradients. However, fossil sites of similar age are located close to each other and the general age trend is such that older sites are from the Western Paratethys and younger sites are from the Eastern part of the region covered. To overcome remaining spatial uncertainties we calculate the paleoprecipitation relative to the present-day values (see below). According to the IPCC, 2007 report, precipitation (relative to recent values) predicted for Europe shows a meridional trend over most of Europe, with little regional variation in the zonal band studied here (Fig. 11.5 in Christensen et al., 2007). Therefore we are confident that our approach of combining data from this area is fairly robust and provides a spatio-temporally coherent record, which is also corroborated by independent coeval proxy data, as discussed further below.

Fossils were derived from a variety of depositional and environmental regimes, like near shore, fluvial, lacustrine and swamp facies and karstic fissure fillings (Supplementary Table 1).

The stratigraphic–chronological framework for the 29 localities (Supplementary Table 1) is based on correlation to local magnetostratigraphically dated sections, sequence- and lithostratigraphic extrapolation, and biostratigraphic correlation.

2.2. Estimation of paleoprecipitation based on herpetofaunal composition

The distribution and spatial occurrence of amphibians and reptiles depend on environmental conditions at various scales, ranging from habitat to global scale (Zug et al., 2001). It is assumed that distribution of species at a given spatial scale is in equilibrium with their environment (Guisan and Theurillat, 2000). Several investigations found a strong positive correlation between annual precipitation and amphibian species richness (e.g. Duellmann, 1999; Duellmann and Sweet, 1999; Tyler, 1994; Crowe, 1990). For reptiles it has been documented that climate (precipitation and temperature) more closely matches their distribution than any other environmental factors such as topography (Guisan and Hofer, 2003; Owen, 1989).
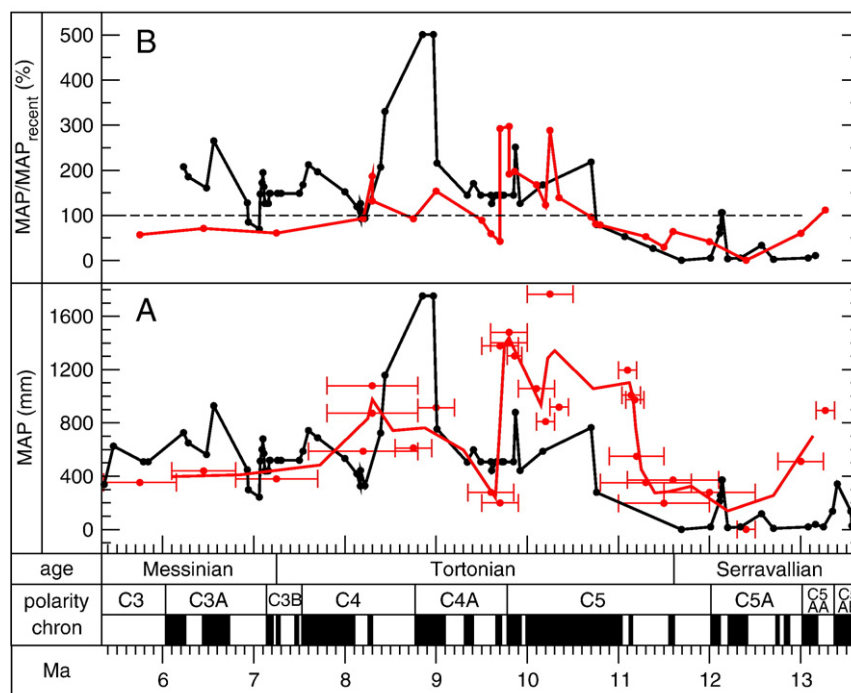
Fig. 2. Serravallian to Messinian precipitation from Europe. A—absolute mean annual precipitation (MAP) values for SW-Europe (black) and Central+Eastern Europe (red, 2-point running mean). B—ratio of MAP relative to recent; 100% means no change relative to recent.

Precipitation serves as a direct predictor for the herpetofaunal distribution and species richness and yields robust and widely applicable modelling results (Austin, 2002). The most important environmental factors for amphibian and reptilian distributions are sunlight availability as the ultimate heat source, and water availability as reproductive- and buffering medium against thermal extremes. Amphibians and reptiles have evolved several different ecophysiological strategies and adaptations to maintain thermoregulation, water balance and gas exchange.

Böhme et al. (2006) assorted recent amphibians and reptiles on the basis of their ecophysiological strategies into six groups. The relative frequency of these groups in recent communities is used to establish an ecophysiological index for communities, which shows a highly significant correlation with mean annual precipitation (r^2=0.88). The correlation was established for a range of recent climatic conditions up to a maximum of 1600 mm annual precipitation. Applying this relationship to fossil communities will yield paleoprecipitation estimates with average errors of ±250 mm for the middle of the range and of ±275 mm for very wet conditions. In the limit of zero precipitation, the 95% prediction interval is from 0 to +275 mm, because precipitation values cannot become negative. Thus, the method is particularly accurate for drought conditions. This paleo-precipitation tool is applicable in fossil assemblages with rich amphibian and reptile records that show relatively low taphonomical bias with respect to the herpetofauna, such as alluvial sediments, paleosoils, caves, fissure fillings, pond and swamp deposits, and channel-fill sediments. It is important to note that, in contrast to paleobotanical methods, this approach is less facies-dependent and applicable to both wet and dry endmembers of the climate system.

For the present investigation we established the database for precipitation estimates from herpetofaunal assemblages (Böhme et al., 2006) using a range-through approach. We follow the methods of Barry et al. (2002) and Van Der Meulen et al. (2005) to estimate the ranges of taxa by closing all gaps shorter than 500 kyr (cf. grey cells in Supplementary Tables 2 A–C and 3A–D). This method assumes that a range gap <500 kyr is due only to sampling and not to emigration of a taxon followed by its immigration. We apply this method consequently

on the Southwest European record, because of the spatially small-scale sampling area (see Section 2.1.1.) and the assumption of a single taphonomic mode bias of the assemblages (Van Der Meulen et al., 2005). The taxon ranges at the old and young end of the data-set are compiled using assemblages from the preceding, respectively following 500 kyr (data not shown here). Because of the larger sampling area and the different depositional regimes in the Central and Eastern Europe data-set we used the range-through approach only in adequate cases (e.g. Hammerschmiede section, Richardhof section).

The resulting data sets (Supplementary Tables 2 and 3) are converted into absolute annual paleoprecipitation estimates using Eq. (6) in Böhme et al. (2006). From the absolute precipitation estimates (Fig. 2A) we calculated the precipitation relative to the present-day values (Fig. 2B) on the basis of actual mean precipitation values from the spatially nearest available climate station of a given fossil locality (Supplementary Table 3E). For the Calatayud–Teruel Basin record we choose the stations of Teruel (Mean Annual Precipitation 373 mm) and Zaragoza (MAP 318 mm) and appreciate a present-day MAP of 350 mm (Supplementary Table 2A–C).

2.3. Estimation of paleorunoff

Combining the precipitation time series from both sectors into a common curve requires a common age model, which however is not the case here. We first have to treat the age uncertainties of the data points from the C+E sector (Paratethys) before we can fit a hypersurface to them, which can then easily be interpolated at the points specified by the good age model for the data from the South-Western sector (Spain). The stochastic ('Boolean') approach to treat the age uncertainties of the data from the C+E sector (see details in online Supplementary Data) transforms error bars in the age model into error bars in precipitation (Fig. 3). After this transformation, the data from the C+E sector can be combined with those of the W-sector to compute the total run-off of both areas. We use the Calatayud–Teruel and the Paratethys precipitation trends (for data see Supplementary Tables 2A–C and 3E) as models for Miocene humidity evolution in the Western and Central+Eastern European sector. The Western sector represents the Iberian Peninsula
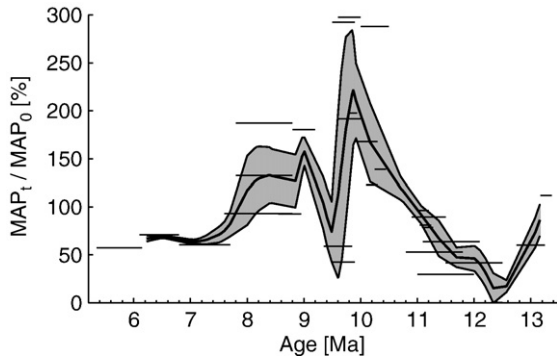
Fig. 3. Ensemble means and ±1σ confidence intervals (grey shaded area) of the relative mean annual precipitation, MAP_t/MAP_0 (×100%) for the C+E sector, obtained from averaging over $N=1000$ random age models, each consistent with the given age uncertainties in the original data-set (red points in Fig. 2B). Horizontal black bars represent the raw data with age uncertainties.

and Western Europe from France up to the Baltic Sea. The Central+ Eastern sector comprises the drainage area of the Adriatic, Black and Caspian Seas. We include the Caspian Sea in this sector because the Caspian and Euxinian (Black Sea) basins were connected during the studied time interval (Popov et al., 2004). On the basis of the present-day catchment area of Europe's 18 largest rivers (Supplementary Table 4) we determine the relative proportion (weight factors) as $w_W=0.3$ and $w_{CE}=0.7$ for the W-sector and the C+E sector, respectively.

For the W-sector, the change in precipitation relative to present-day values, $\Delta MAP = MAP_t - MAP_0$ (in mm), and the precipitation ratio MAP_t/MAP_0 (×100%) (note that $MAP_t/MAP_0 = 1 + \Delta MAP/MAP_0$) show exactly the same variation since the W-sector is represented by the Calatayud–Teruel Basin with a single MAP_0 of 350 mm. ΔMAP and MAP_t/MAP_0 for the C+E sector show a very similar variation since MAP_0 does not vary much among most locations from the C+E sector, except for location "Hammerschmiede", which represents the pre-

cipitation model for the range of 11.1–11.2 Ma (Fig. 2). With this good agreement between ΔMAP and MAP_t/MAP_0, we can use MAP_t/MAP_0 to compute the relative change in run-off from relative to recent values by applying the empirical relationship established by Karl and Riebsame (1989).

$$\log_{10}\left(\frac{R_t}{R_0} \cdot 100\%\right) = b + m \cdot \log_{10}\left(\frac{MAP_t}{MAP_0} \cdot 100\%\right) \quad (1)$$

where MAP and R denote mean annual precipitation and run-off, respectively, at time t in the past and today (subscript 0). The empirical slope m is 2.11, and the offset b is obtained as −2.22 from the relation $b=2*(1-m)$. Note that the effects of evapotranspiration are implicitly included in the relationships. Higher precipitation is coupled with higher cloud cover, which reduces evaporation.

It is important to note that Karl and Riebsame (1989) established the relationship for maximum precipitation ratios of 1.75, leading to an amplification of 3.1 (e.g., 75% more rainfall leads to 230% more run-off). While the precipitation ratios in the C+E sector do not exceed 2.0, the positive rainfall anomalies in the W-sector may reach 4.0 and therefore would yield an amplification of 6. Rather than to extrapolate the amplification on the basis of Eq. (1) for MAP_t/MAP_0 ratios greater than 1.75 (which is beyond the data basis for the empirical precipitation–run-off relationship), we limit the maximum amplification factor to 3.1.

Najjar (1999) analyzed the water balance of the Susquehanna River Basin (Chesapeake Bay) over the last 100 yr and found a mean amplification factor of 2. The total run-off at time t in the past, R_t (Fig. 4) is obtained as the weighted sum of the run-off curves of each sector,

$$R_t = R_0 \cdot \left(w_W \left.\frac{R_t}{R_0}\right|_W + w_{CE} \left.\frac{R_t}{R_0}\right|_{CE} \right) \quad (2)$$

where the respective run-off-ratios are computed according to Eq. (1). According to Oki (2001) the present-day European run-off is
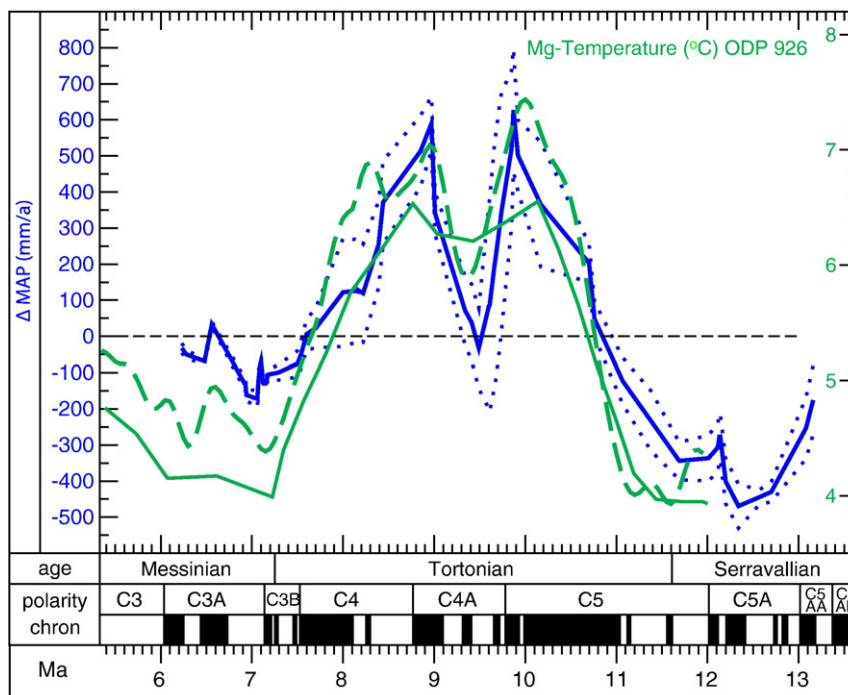
Fig. 4. Weighted European precipitation curve relative to recent (blue), with 1σ intervals (for more information see Supplementary Data, Sections 3–5), green dashed line—Ceará Rise deep-water temperature ($T_{926}^{Mg/Ca}$) derived from Mg to Ca ratios in benthic foraminifers (*C. mundulus, O. umbonatus*) from the eastern equatorial Atlantic (ODP Site 926, Lear et al., 2003, green solid line—smoothed $T_{926}^{Mg/Ca}$, based on three species, *C. mundulus, O. umbonatus, C. wuellerstorfi* (10% weighted fit, see Fig. 6 in Lear et al., 2003.)

$R_0 = 1.7 \times 10^{15}$ kg/a, which corresponds to 0.054 Sv (1 Sv = 10^6 m^3/s), see Supplementary Table 4.

3. Results

The precipitation proxy record for Southwest Europe (black curve in Fig. 2A) shows frequent high-amplitude changes during the studied interval. For most of the Tortonian, MAP is generally estimated to be higher than present-day values, but lower MAP was estimated for the Serravallian. Most notably, an unprecedentedly wet episode occurred between 9.2 and 8.5 Ma, with up to 5 times higher MAP than present. The MAP proxy record for Central to Eastern Europe (red curve in Fig. 2A) is a composite from different locations (older sites in the Western part of the Paratethys region, younger sites in the central part), with different present-day MAP values. A clearer picture therefore emerges when the paleoMAP estimates are divided by the respective present-day MAP values (Fig. 2B). Both of the so obtained relative MAP curves reveal significantly drier than present conditions between 13.2 and 11.5 Ma (Serravallian), with typically less than 50% precipitation compared to recent. This dry interval represents the most intense and prolonged arid period in Europe since the middle Miocene climatic optimum (Böhme, 2003). Positive rainfall anomalies on the other hand were most pronounced during the Tortonian, between 10.7 and 9.7 Ma (Central to Eastern Europe) and at 8.9 Ma (SW-Europe), when the amount of rainfall exceeded present-day values by more than 200%, indicating a substantial intensification of the hydrological cycle. Such conditions in warm extratropical climates when precipitation was more than doubled compared to today can be considered as washhouse climate. The precipitation trends in Southwest and Central to Eastern Europe are positively correlated for the late middle to early late Miocene.

From the late Tortonian onward (after 8 Ma), the precipitation curves for the Southwest sector still shows variability with significantly more humid values than present-day, while the one for the Paratethys consistently remains below present-day values, which is in agreement with the spread of steppe biomes at that time in Eastern Europe (Velichko et al., 2005; Eronen, 2006). Nevertheless, the overall cross-correlation value between the two time series displayed in Fig. 2B amounts to 0.85 (maximum for zero-lag time).

Our precipitation trends for Central to Eastern Europe are strongly supported by paleontological and stable-isotope studies from the large Central Paratethyan Lake Pannon (Harzhauser et al., 2007). The long dry interval at the beginning of our record, which is derived from sites from the Western Paratethys and western side of the Central Paratethys, is also reflected by elevated salinities in Lake Pannon at around 11.6 Ma. The salinity of the lake decreased steadily until 10 to ~9.5 Ma, the time of its maximum depth and horizontal extension, which tallies with the strong increase in our precipitation record for the C+E sector (Fig. 3). The freshening and increase in lake level were interpreted as a result of increasing summer precipitation (Harzhauser et al., 2007). Similar to our results, paleobotanical and mammalian proxy data also indicate mean annual precipitation of around 1.200 mm in the locality Rudabanya (Hungary), north of the Lake Pannon, for the time around 10 Ma (Bernor et al., 2003).

4. Discussion

4.1. Consequences for ecosystem dynamics in continental Europe

Importantly, the change from wetter to dryer climate between 9.7 and 9.5 Ma is coeval with a change from evergreen to deciduous vegetation in Spain and supposed to be associated with the extinction of hominoids in Western Europe, known as the Vallesian crisis in mammal paleontology (Agusti et al., 2003). We propose that the significant decrease in the intensity of the hydrologic cycle between 9.7 and 9.5 Ma is a plausible explanation for this ecosystem crisis. The waning of evergreen forests due to decreased precipitation in turn reduced the survival ability of frugivorous animals such as hominoids, which rely on high quantities of glucose-rich food throughout the year to sustain their elevated brain metabolism. Other forest-dwellers are eventually supplanted by grassland species invading from Eastern Europe, together with the spread of Steppe biomes.

4.2. Comparison with marine proxy data

A remarkable correlation is apparent (Figs. 4 and 5A) between the European water cycle record and an Atlantic deep-water temperature proxy record ($T_{926}^{Mg/Ca}$) constructed by Lear et al. (2003) using benthic foraminiferal Mg/Ca ratios from Ceará Rise, ODP Site 926 (4°N, 43°W), water depth 3500 m. Today, the site is in the mixing zone between North Atlantic Deep Water (NADW) and Antarctic Bottom Water (AABW) and considered to have archived past variations in the flow of proto-NADW (ancient NADW, devoid of a Middle NADW contribution from the Labrador Sea) and return flow of water masses of Antarctic origin (southern sourced water). Most importantly, the $T_{926}^{Mg/Ca}$ curve shows a positive double-peak anomaly of 2.5–3 °C, which coincides with the two washhouse intervals (Fig. 4). Lear et al. (2003) offered two possible interpretations for the positive $T_{926}^{Mg/Ca}$ excursions in the interval of 8–10 Ma, either a vertical movement of water masses, or a reduction of proto-NADW flow and replacement by warmer water masses of Antarctic origin. However, if reduction of proto-NADW was to be responsible for the $T_{926}^{Mg/Ca}$ anomaly, we would expect to see another pronounced $T_{926}^{Mg/Ca}$ anomaly developing at about 7.5 Ma, when proto-NADW flux as is waning even more (Fig. 5C), as indicated by decrease in Northern Component Water (NCW) proxy record constructed on the basis of spatial gradients in the divergence of benthic carbon isotope records (Wright and Miller, 1996; Poore et al., 2006). Yet, the $T_{926}^{Mg/Ca}$ record obviously remains unaffected by the substantially weakening NCW flow from 8 Ma to 7 Ma. Nor does the European run-off record seem to be correlated with NCW fluctuations over the whole time interval studied. It rather appears that NCW flow (perhaps beyond some threshold strength) is one necessary condition for a European washhouse climate to occur, while higher temperatures, at least in the North Atlantic domain, are another necessary condition, although both conditions are not necessarily sufficient and not independent of each other, since higher sea-surface temperatures in the North Atlantic not only lead to greater evaporation, but also via higher salinities to an intensification of the thermohaline branch of the Atlantic Meridional Overturning Circulation (AMOC). In turn, an intensified thermohaline circulation delivers more heat (and moisture) to the mid- and high northern latitudes. Available proxy data (Kaminski et al., 1989; Helland and Holmes, 1997; Duncan and Helgason, 1998; Thiede et al., 1998; Billups and Schrag, 2002; John and Krissek, 2002; Diekmann et al., 2003; Westerhold et al., 2005) suggest that also global temperatures were higher when the washhouse regime reigned over Europe. Globally higher temperatures would have warmed both the North Atlantic and Antarctic, causing the $T_{926}^{Mg/Ca}$ double peak in the time interval between 10 and 8 Ma, independent of whether the temperature anomaly was advected to ODP site 926 by proto-NADW flow or by a return flow of Antarctic origin.

Interestingly, despite low activity of the Iceland plume around 16 Ma (Wright and Miller, 1996), spatial gradients in the benthic carbon isotopes before 12 Ma are too small to yield robust estimates of NCW (Poore et al., 2006), which may indicate that NCW flow was poorly developed before 12 Ma. Winkler et al. (2002) observed a change in clay mineral ratios and bulk sediment accumulation rate at around 11.2 Ma (Fram Strait, off the western coast of Spitzbergen), which they attribute to a change in provenance, an increase in water-mass exchange through the Fram Strait, and possibly an intensification of the Atlantic circulation. Neodymium isotopes studies on slowly growing ferromanganese crusts indicate a strong overall export of NADW (or a precursor of it) already since 14 Ma (Frank et al., 2002). Taken together, these observations suggest—despite some unresolved
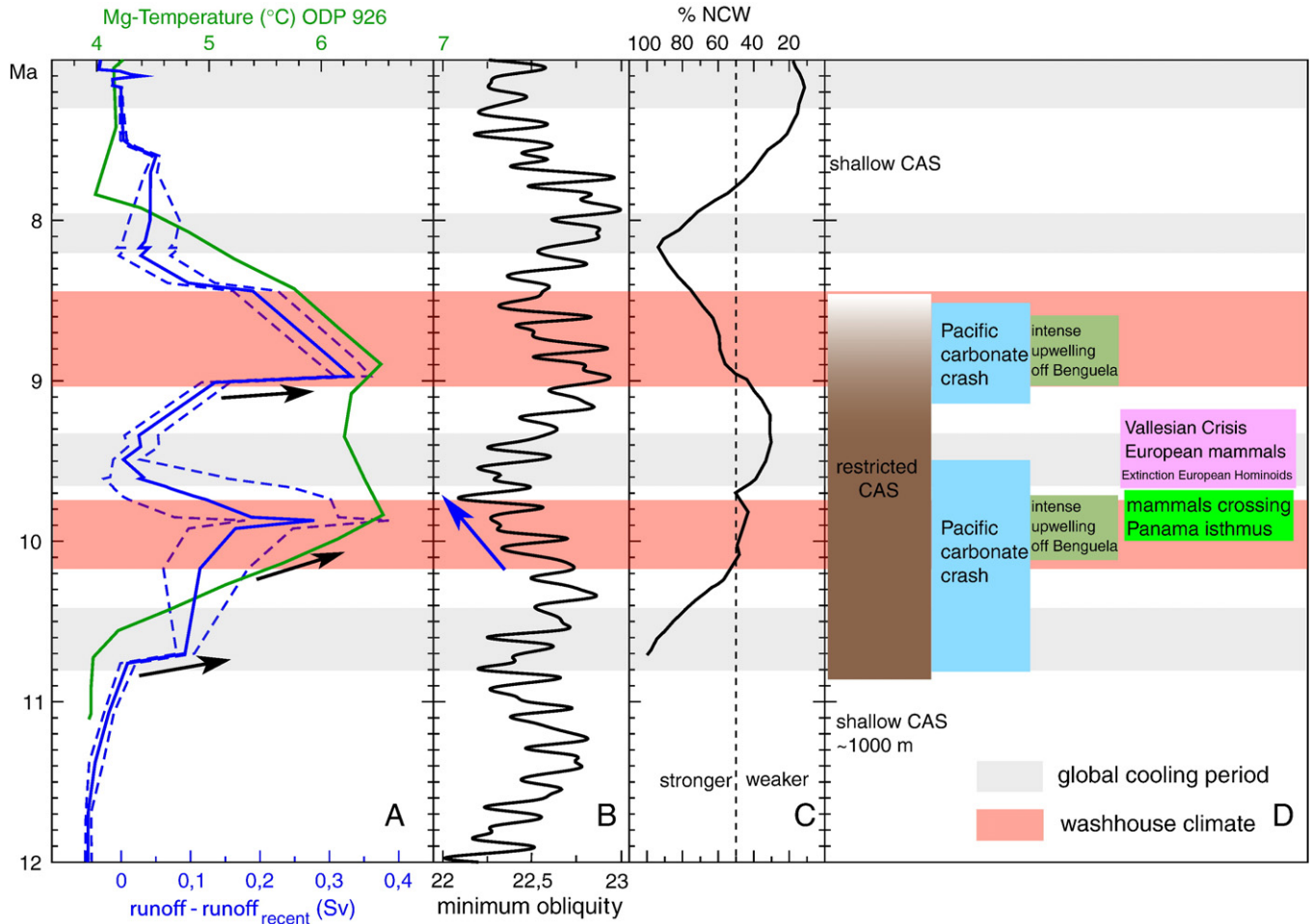
Fig. 5. Events associated with the Tortonian temporary closure of the Panama Isthmus. Horizontal bars: Washhouse climate in Europe (magenta); global cool periods (grey) (Kaminski et al., 1989b; Helland and Holmes 1997; Duncan and Helgason 1998; Thiede et al., 1998; Billups and Schrag 2002; John and Krissek 2002; Diekmann et al., 2003; Westerhold et al., 2005). A—Estimated European freshwater run-off in Sv (1 Sv=10^6 m^3 s^−1) relative to recent (blue) and $T_{926}^{Mg/Ca}$ (green) as in Fig. 4; black arrows indicate periods of enhanced moisture transport into high northern latitudes. B—lower envelope of obliquity (Laskar et al., 2004); the decrease in tilt angle causes increasingly cool summers at high latitudes (blue arrow). C—Variation of Northern Component Water (NCW=proto-NADW) from Poore et al. (2006); "stronger" and "weaker" refer to the present day (dashed line). D—brown: Closing history of the Central American Seaway (CAS) according to Kameo and Sato (2000); blue: timing of the most severe Pacific carbonate crash episodes (Lyle et al., 1995; Roth et al., 2000); light green: periods of intense upwelling off Benguela as indicated by nanoplankton productivity (Kastanja et al., 2006; Krammer et al., 2006); dark green: timing of the first Great American Biotic Interchange Marshall, 1985; magenta: Vallesian crisis in European mammals (Agusti et al., 2003).

discrepancies—that North Atlantic deep-water formation and over-turning circulation were already developed during the time of the washhouse climate in Europe. The different nature, sensitivity, and temporal resolution of the proxy records used for proto-NADW production/export makes it difficult to better constrain its potential impact on Tortonian European climate.

4.3. Freshwater forcing

Besides tectonic mechanisms, freshwater forcing during periods of washhouse climate may have affected NCW formation as well. Of course, this discussion has to remain on the conceptual level for the lack of comparable proxy data from other regions of the North Atlantic catchment area. The European run-off estimated here is discharged into the North Atlantic at moderate latitudes and feeds into the subtropical gyre, whose northward branch merges with the Gulf Stream. However, since the North Atlantic is the primary source of precipitation in Europe, the hydrological balance can be expected to be in equilibrium and the net change in freshwater forcing is practically zero. This is the key difference to rapid meltwater pulses that strongly perturb a hydrological equilibrium state of the AMOC, which may lead to complete shutdown of NADW flow with transiently non-reversible (hysteretical) behaviour (Rahmstorf, 1996).

Nevertheless, there is a possible, indirect scenario that may result in freshwater forcing of the North Atlantic during the washhouse period, through freshening the Arctic Ocean by enhanced Siberian river run-off. This is in as much an option as our precipitation data for the Paratethys region (Central Europe) might also be representative of the precipitation trends in the West Siberian river system, which exports moisture out of the North Atlantic catchment area into the Arctic Ocean. Enhanced Siberian river discharge promotes stratification in the Greenland–Norwegian Sea and so counteracts overturning and NADW formation (Peterson et al., 2002). Interestingly, the strong increase in precipitation from 11 to 9.8 Ma in Central Europe (Fig. 3) is coincident with a decrease in NCW (Fig. 5C). However, due to the lack of direct West Siberian precipitation data in this period we are not in a position to quantify the corresponding freshwater forcing.

4.4. Possible mechanisms

The reasons for the pronounced variations in the hydrological cycle of Southwest and Central Europe are elusive, particularly so for the two several hundred kyr long washhouse periods, which seem unexampled in the younger Earth's history. From the comparison with other proxy data, we have concluded in Section 4.2 that washhouse situations are promoted by warm conditions in the North Atlantic domain and by

proto-NADW production above a certain threshold level. Evidently, these constraints lead to more evaporation over the North Atlantic, which is the preponderant source of European precipitation. On the other hand, there have been times when both conditions were met without there being a washhouse climate in Europe, which renders these conditions merely necessary, but not sufficient. There may well have been feedback mechanisms at work, due to enhanced greenhouse forcing by methane produced in wetlands or by atmospheric water vapour, or due to more lush vegetation under wet climates.

Possible vegetation-climate feedback mechanisms for a typical late Miocene vegetation cover have already been studied (Brachert et al., 2006; Lohmann et al., 2006), albeit in different contexts. Brachert et al. (2006) used a complex atmospheric general circulation model coupled to an adjusted surface mixed-layer ocean model, applied to an early Tortonian vegetation scenario with larger forest cover than today and an ice-free Greenland. Compared to present-day winter conditions, the Icelandic Low in the model is found to be displaced southwards and more pronounced relative to the Azores High and thus transports mild and moist air from the Atlantic to the Mediterranean. That study was mainly concerned with explaining interannual variability and assumed recent land–sea distribution, with generally lower orography than present. Since long-term climatic changes were not relevant in Brachert et al. (2006), it was justified to use a simplified ocean model that did not allow for deep-water formation and overturning circulation. Lohmann et al. (2006), integrating over longer timescales and including the deep ocean within a general ocean-circulation model, focussed on the feedback between vegetation cover and oceanic circulation. A scenario with lush vegetation cover, deemed characteristic of the Tortonian, and an open Central American Seaway (CAS) was found to lead to higher evaporation over the North Atlantic Ocean, which intensifies the thermohaline branch of the AMOC and therefore compensates for the otherwise adverse effects of an open CAS on the AMOC. Lohmann et al. (2006) also obtained a pronounced change in the global distribution of annual mean net precipitation (precipitation minus evaporation), but the changes predicted for Southwest and Central Europe are relatively modest compared to those predicted for low latitudes and the North Atlantic. Therefore, that modelling study does not point to a washhouse climate, and it would be interesting to see the differences obtained for a Tortonian vegetation scenario with a CAS restricted to large-scale oceanic exchange, a situation for which there is some evidence as we shall discuss in the next section.

4.5. Possible role of a temporary restriction of the Central American Seaway in the Miocene

Interestingly, the two periods of washhouse climate are roughly coeval with two major carbonate crash episodes reported for the tropical eastern Pacific Ocean (Fig. 5A and D), which were interpreted to have been caused by a loss of alkaline Atlantic waters, most likely in response to a constriction of the Central American Seaway (CAS), which would have restricted the flow of relatively high alkalinity waters from the Atlantic to the eastern Pacific (Lyle et al., 1995; Roth et al., 2000). In the following, we explore the possible role that a restriction of the CAS in the Miocene might have had on European climate. It has been repeatedly suggested that the final closure of the CAS in the Pliocene could have caused a reorganization of oceanic and atmospheric circulation, which in turn might have facilitated or even triggered the growth of ice sheets in the Northern hemisphere (Keigwin, 1982; Driscoll and Haug, 1998; Bartoli et al., 2005), although others have argued that CAS closure rather delayed the Ice Age (Berger and Wefer, 1996, see also Molnar, 2008 for a critical review). To begin with, we summarize the lines of evidence for a temporary restriction of the CAS in the Miocene, and then discuss its possible connection to the European washhouse climate.

During most of the Miocene an open CAS allowed for the exchange of saline Atlantic waters with less saline Pacific waters (e.g., Keigwin,

1982). In the late middle Miocene, however, a major tectonic uplift of Panama led to shoaling of the CAS up to middle-bathyal depth of ∼1000 m (Duque-Caro, 1990; Coates et al., 2003), which still enabled the Circum-tropical Current to flow across. As depicted in Duque-Caro (1990) and Kameo and Sato (2000), the CAS during that time can be thought of as an archipelago, in some way analogous to the present-day Indonesian seaway. However, the divergence between coccolithophore assemblages on either side of the CAS between 10.89 and 8.29 Ma[1] indicates that the Atlantic–Pacific surface water exchange was temporarily restricted (Kameo and Sato, 2000; Roth et al., 2000), which is also supported by the first intercontinental exchange of terrestrial mammalian taxa (e.g., the sloth *Pliometanastes*) at the base of the Hemphillian North American Land Mammal Age (Lindsay et al., 1984; Marshall, 1985), which has been magnetostratigraphically assigned to Chron C4Ar2n (∼9.8 Ma) (Whistler and Burbank, 1992).

Since the initial work by Maier-Reimer et al. (1990) various numerical modelling studies have been performed to assess the effects of the Pliocene CAS closure on ocean circulation and most models suggest that closure (and even shoaling) of the CAS enhances the Atlantic thermohaline circulation (for recent reviews, see Molnar, 2008 and Lunt et al., 2008b). Using a coupled ocean–sea-ice–atmosphere model, Prange and Schulz (2004) investigated the effects of CAS closure on northward heat transport in the Atlantic Ocean and associated changes in the subtropical high pressure systems. According to that sensitivity study, CAS closure induces a large-scale redistribution of heat in the Atlantic such that the meridional oceanic heat transport in the South Atlantic becomes northward directed (as is the situation today). Compared to the open CAS scenario, the Azores High now weakens, whilst the subtropical high pressure system over the South Atlantic intensifies. This reinforces the southern trade winds, leading to enhanced upwelling off Southwest Africa, a pattern, which is suggested by several proxy data from the Benguela system (Kastanja et al., 2006; Krammer et al., 2006) during times of a temporarily restricted CAS (see Fig. 5, right column).

The strength of the subtropical high pressure system centered over the Atlantic off Portugal (Azores High) has a large influence on European precipitation. A weak Azores High allows cold fronts from the Icelandic Low pressure system to sweep across moderate latitudes of continental Europe, and conversely, a pronounced Azores High deflects storms on more northerly tracks. Thus, a relatively weak Azores High in the restricted CAS scenario would lead to a southward shift of westerly winds and associated storm tracks. Invoking the atmospheric pressure seesaw mechanism, we can explain the arid-to-humid transition in our proxy record in the earliest Tortonian, by linking the negative precipitation anomaly in the late Serravallian to a strong Azores High under open CAS conditions, and conversely, the positive precipitation anomaly in the Tortonian to a reduced Azores High in a restricted CAS scenario. A consistently stronger Azores High in the relatively dry interval between 13 and 11 Ma further implies that Northern Europe would have been wetter during that interval due to the northward shift of storm tracks, but precipitation proxy data are not available to test this proposition. Likewise, intensified upwelling off Northwest Africa would be expected under this scenario, but no data-set exists yet to proof or disprove the proposed upwelling seesaw mechanism.

A consistently weaker Azores High in the humid period, of course, does not automatically imply a washhouse climate. However, we need to point out that the washhouse periods occurred in a warm world with several °C higher global average temperatures than today, implying a much higher atmospheric moisture content, which we believe can make all the difference compared to present. We strongly encourage modelling studies to further explore the magnitude of this possible teleconnection for a 'warm ocean' scenario and its impact on atmospheric circulation and to provide predictions that can be related

---

[1] All ages recalibrated after the Geological Time Scale 2004.

directly to proxy data (e.g. changes in precipitation, in physical bottom water temperatures). With the presently available marine proxy data, we are not in a position yet to provide more evidence for our hypothesis that the temporary restriction of the CAS was a necessary condition for the European washhouse climate. Of course, one can always argue that the coeval occurrence of two events may be purely coincidental without a physical connection.

4.6. Role of washhouse climate on glaciations

During the time interval of a temporarily restricted CAS, enhanced run-off is correlated with times of warm climate periods, that is, when ocean temperatures are increased relative to Miocene cool periods, leading to high evaporation. Similarly, the period of relatively low precipitation between 9.7 and 9.2 Ma corresponds to a global cool event (e.g. Winkler et al., 2002; Diekmann et al., 2003; Westerhold et al., 2005), which is also documented by a change in coiling of *Neogloboquadrina* south of Greenland (Kaminski et al., 1989). The cool event was probably triggered by the increasing amplitude of obliquity (Fig. 5B), which led to cooler summers at high latitudes with decreasing tilt angle and build-up of the South Greenland ice sheets under ongoing atmospheric moisture transport. This situation is remarkably similar to what has been inferred for the final closure of the CAS in the Pliocene (Driscoll and Haug, 1998; Bartoli et al., 2005).

5. Conclusions

Based on the relative frequencies of herpetofaunal groups, we have constructed two eight-million year long precipitation proxy records for Southwestern and Central to Eastern Europe in the late middle and late Miocene (13.5–5.5 Ma) with mean temporal resolution of ~60 kyr and ~150 kyr, respectively. The records reveal two episodes of anomalously high precipitation, coeval with global warm periods as indicated by marine and other continental climate proxy records. We refer to such climatic conditions in moderate latitudes as washhouse climate. The reasons for the washhouse climate remain enigmatic for the lack of a suitable present-day analogue.

We conjecture that the temporarily constricted Central America Seaway (CAS), which restricted the exchange of water masses between the tropical Atlantic and Pacific oceans and most likely affected the northward heat transport, set the scene for the enhanced hydrological cycle in Europe, induced by overall higher sea-surface temperatures during global warm periods, with possible feedback-mechanism mediated by a lush vegetation cover and greenhouse forcing due to water vapour and methane produced in wetlands. Indirect evidence for this conjecture is furnished by an 'evidence of absence' type of argument: The precipitation record reveals no other washhouse periods during any of the warm periods before or after the temporary restriction of the CAS in the Miocene.

Lastly, our results indicate that under warm ocean conditions, a washhouse climate in Europe may well represent a possible scenario for future global warming. On the basis of a coupled ocean–atmosphere–land model, it was predicted that the hydrological cycle would significantly intensify in response to global warming (Manabe et al., 2004). A quadrupling of the atmospheric carbon dioxide concentration was found to entail an increase in North Atlantic surface temperatures of up to 6 °C and an enhanced tropospheric poleward moisture transport (Manabe and Stouffer, 1994), resulting in up to 60% more run-off for individual mid-latitude drainage systems (Manabe et al., 2004). Our results demonstrate that changes in the hydrological cycle are probably one of the strongest forces driving ecosystem dynamics during the late Miocene.

Acknowledgements

Appendix A. Supplementary data

Supplementary data associated with this article can be found, in the online version, at doi:10.1016/j.epsl.2008.09.011.

References

Abdul Aziz, H., Van Dam, J., Hilgen, F.J., Krijgsman, W., 2004. Astronomical forcing in Upper Miocene continental sequences: implications for the Geomagnetic Polarity Time Scale. Earth Planet. Sci. Lett. 222, 243–258.

Agusti, J., Sanz de Sira, A., Garcés, M., 2003. Explaining the end of the hominoid experiment in Europe. J. Hum. Evol. 45, 145–153.

Austin, M.P., 2002. Spatial prediction of species distribution: an interface between ecological theory and statistical modelling. Ecol. model. 157, 101–118.

Barry, J.C., Morgan, M.E., Flynn, L.J., Pilbeam, D., Behrensmeyer, A.K., Mahmood, A.S., Khan, I.A., Badgley, C., Hicks, J., Kelly, J., 2002. Faunal and environmental change in the late Miocene Siwaliks of northern Pakistan. Palaeobiol. Mem. ((suppl.) 3), 1–71.

Bartoli, G., Sarnthein, M., Weinelt, M., Erlenkeuser, H., Garbe-Schönberg, D., Lea, D.W., 2005. Final closure of Panama and the onset of northern hemispheric glaciation. Earth Planet. Sci. Lett. 237, 33–44.

Berger, W.H., Wefer, G., 1996. Expeditions in the past: paleoceanographic studies in the South Atlantic. In: Wefer, G.E.A. (Ed.), The South Atlantic: Present and Past Circulation. Springer, Berlin, pp. 363–410.

Bernor, R., Kordos, L., Rook, L., Agusti, P.A.J., Armour-Chelu, M., Begun, D., Cameron, D., Daxner-Hoeck, G., Bonis, L.D., Damuth, J., Fejfar, O., Fessaha, N., Fortelius, M., Franzen, J., Gasparik, M., Gentry, A., Heissig, K., Hernyak, G., Kaiser, T., Koufos, G., Krolopp, E., Janossy, D., Llenas, M., Meszaros, L., Mueller, P., Renne, P., Rocek, Z., Sen, S., Scott, R., Szyndlar, Z., Tupal, G., Dam, J.V., Werdelin, L., Ungar, P.S., Ziegler, R., 2003. Recent advances on multidisciplinary research at Rudabanya, Late Miocene (MN9), Hungary: a compendium. Palaeontogr. Ital. 89, 3–36.

Billups, K., Schrag, D.P., 2002. Paleotemperatures and ice volume of the past 27 Myr revisited with paired Mg/Ca and 18O/16O measurements on benthic foraminifera. Paleoceanography 17, 26–37.

Böhme, M., 2003. Miocene climatic optimum: evidence from lower vertebrates of Central Europe. Palaeogeogr. Palaeoclimatol. Palaeoecol. 195, 389–401.

Böhme, M., Ilg, A., Ossig, A., Küchenhoff, H., 2006. A new method to estimate paleoprecipitation using fossil amphibians and reptiles and the Middle and Late Miocene precipitation gradients in Europe. Geology 34, 425–428.

Brachert, T.C., Reuter, M., Felis, T., Kroeger, K.F., Lohmann, G., Micheels, A., Fassoulas, C., 2006. Porites corals from Crete (Greece) open a window into Late Miocene (10 Ma) seasonal and interannual climate variability. Earth Planet. Sci. Lett. 245, 81–94.

Bruch, A.A., Utescher, T., Mosbrugger, V., Gabrielyan, I., Ivanov, D.A., 2006. Late Miocene climate in the circum-Alpine realm — a quantitative analysis of terrestrial paleofloras. Palaegeogr. Palaeoclimatol. Palaeoecol. 238, 270–280.

Christensen, J.H., 2007. Regional climate projections. In: Solomon, S., Qin, D., Manning, M. (Eds.), Climate Change 2007: The Physical Science Basis. . Contribution of Working Group I to the Fourth Assessment Report of the Intergovernmental Panel on Climate Change. Cambridge University Press, Cambridge, UK.

Coates, A.G., Aubry, M.P., Berggren, W.A., Collins, L.S., Kunk, M., 2003. Early Neogene history of the Central American arc from Bocas del Toro, western Panama. Geol. Soc. Am. Bull. 115, 271–287.

Crowe, T., 1990. A quantitative analysis of patterns of distribution, species richness and endemism in South African vertebrates. In: Peters, G., Hutterer, R. (Eds.), Vertebrates in the Tropics. Alexander Koenig Zoological Research Institute and Zoological Museum, Bonn, pp. 145–160.

Daams, R., van der Meulen, A., Alvarez Sierra, M.A., Peláez-Campomanes, P., Krijgsman, W., 1999. Aragonian stratigraphy reconsidered, and a re-evaluation of the middle Miocene mammal biochronology in Europe. Earth Planet. Sci. Lett. 165, 287–294.

Diekmann, B., Fälker, M., Kuhn, G., 2003. Environmental history of the south-eastern South Atlantic since the Middle Miocene: evidence from the sedimentological records of ODP Sites 1088 and 1092. Sedimentology 50, 511–529.

Driscoll, N.W., Haug, G., 1998. A short circuit in thermohaline circulation: a cause for Northern Hemisphere glaciation? Science 282, 436–438.

Duellmann, W.E., 1999. Distribution patterns of amphibians in South America. In: Duellman, W.E. (Ed.), Patterns of Distribution of Amphibians — A Global Perspective. John Hopkins University Press, Baltimore, pp. 255–328.

Duellmann, W.E., Sweet, S.S., 1999. Distribution patterns of amphibians in the nearctic region of North America. In: Duellman, W.E. (Ed.), Patterns of Distribution of Amphibians — A Global Perspective. John Hopkins University Press, Baltimore, pp. 31–109.

Duncan, R.A., Helgason, J., 1998. Precise dating of the Holmatindur cooling event in eastern Iceland: evidence for mid-Miocene bipolar glaciation. J. Geophys. Res. B 103, 12397–12404.

Duque-Caro, H., 1990. Neogene stratigraphy, paleoceanography and paleobiogeography in the northwest South America and the evolution of the Panama sea-way. Palaeogeogr., Palaeoclimatol., Palaeoecol. 77, 203–234.

Eronen, J., 2006. Eurasian Neogene large herbivore mammals and climate. Acta Zool. Fenn. 216, 1–72.

Frank, M., Whitely, N., Kasten, S., Hein, J.R., O'Nions, K., 2002. North Atlantic Deep Water export to the Southern Ocean over the past 14 Myr: evidence from Nd and Pb isotopes in ferromanganese crusts. Paleoceanography 17 10.1029/2000PA000606.

Guisan, A., Hofer, U., 2003. Predicting reptile distributions at the mesoscale: relation to climate and topography. J. Biogeogr. 30, 1233–1243.

Guisan, A., Theurillat, J.P., 2000. Equilibrium modeling of alpine plant distribution and climate change: how far we can go? Phytocoenologia 30, 353–384.

Harzhauser, M., Latal, C., Piller, W.E., 2007. The stable isotope archive of Lake Pannon as a mirror of Late Miocene climate change. Palaeogeogr. Palaeoclimatol. Palaeoecol. 249, 335–350.

Helland, P.E., Holmes, M.A., 1997. Surface textural analysis of quartz sand grains from ODP Site 918 off the southeast coast of Greenland suggest glaciations of southern Greenland at 11 Ma. Palaeogeogr. Palaeoclimatol. Palaeoecol. 135, 109–121.

IPPC, 2007. The physical science basis. In: Solomon, S., Qin, D., Manning, M., et al. (Eds.), Climate Change 2007. . Contribution of Working Group I to the Fourth Asessment Report of the Intergovernmental Panel on Climate Change. Cambridge University Press, UK.Cambridge, p. 996.

John, K.E.K., Krissek, L.A., 2002. The late Miocene to Pleistocene ice-rafting history of southeast Greenland. Boreas 31, 28–35.

Kameo, K., Sato, T., 2000. Biogeography of Neogene calcareous nannofossils in the Caribbean and the eastern Pacific – floral response to the emergence of the Isthmus of Panama. Mar. Micropaleontol. 39, 201–218.

Kaminski, M.A., Gradstein, F.M., Scott, D.B., Mackinnon, K.D., 1989. Neogene benthic foraminifer biostratigraphy and deep-water history of Sites 645, 646 and 647, Baffin Bay and Labrador Sea. In: Srivastava, S.P., Arthur, M., Clement, B. (Eds.), Proceedings of the Ocean Drilling Program, Scientific Results. Ocean Drilling Program, College Station, TX, pp. 731–756.

Karl, T.R., Riebsame, W.E., 1989. The impact of decadal fluctuations in mean precipitation and temperature on runoff: a sensitivity study over the United States. Clim. Change 15, 423–447.

Kastanja, M.M., Diekmann, B., Henrich, R., 2006. Controls on carbonate and terrigenous deposition in the incipient Benguela upwelling system during the middle to the late Miocene (ODP Sites 1085 and 1087). Palaeogeogr. Palaeoclimatol. Palaeoecol. 241, 515–530.

Keigwin, L., 1982. Isotopic paleoceanography of the Caribbean and East Pacific: role of Panama Uplift in Late Neogene Time. Science 217, 350–353.

Krammer, R., Baumann, K.H., Henrich, R., 2006. Middle to Late Miocene fluctuations in the incipient Benguela upwelling system revealed by coccolith assemblages (ODP Site 1085A). Palaeogeogr. Palaeoclimatol. Palaeoecol. 230, 319–334.

Laskar, J., Robutel, P., Joutel, F., Gastineau, M., Correia, A.C.M., Levrard, B., 2004. A long term numerical solution for the insolation quantities of the Earth. Astron. Astrophys. 428, 261–285.

Lear, C.H., Rosenthal, Y., Wright, J.D., 2003. The closing of a seaway: ocean water masses and global climate change. Earth Planet. Sci. Lett. 210, 425–436.

Lindsay, E.H., Opdyke, N.D., Johnson, N.M., 1984. Blancian–Hemphillian land mammal ages and late Cenozoic mammal dispersal events. Annu. Rev. Earth Planet. Sci. 12, 445–488.

Lohmann, G., Butzin, M., Micheels, A., Bickert, T., Mosbrugger, V., 2006. Effect of vegetation on the Late Miocene ocean circulation. Clim. Past Discuss 2, 605–631.

Lunt, D.J., Flecker, R., Valdes, P.J., Salzmann, U., Gladstone, R., Haywood, A.M., 2008a. A methodology for targeting palaeo proxy data acquisition: a case study for the terrestrial late Miocene. Earth Planet. Sci. Lett. 271, 53–62.

Lunt, D.J., Valdes, P.J., Haywood, A., Rutt, I.C., 2008b. Closure of the Panama Seaway during the Pliocene: implications for climate and Northern Hemisphere glaciation. Clim. Dyn. 30, 1–18.

Lyle, M., Dadey, K.A., Farrel, J.W., 1995. The late Miocene (11 – 8 Ma) eastern Pacific carbonate crash: evidence for reorganisation of deep-water circulation by the closure of the Panama gateway. In: Pisias, N., Mayer, L., Janecek, T., Palmer-Julson, J., van Andel, T. (Eds.), Proceedings ODP Scientific Results. Ocean Drilling Program, College Station, TX, pp. 821–838.

Maier-Reimer, E., Mikolajewicz, U., Crowley, T.J., 1990. Ocean General Circulation Model sensitivity experiment with an open Central American Isthmus. Paleoceanography 5, 349–366.

Manabe, S., Stouffer, R.J., 1994. Multiple-century response of a coupled ocean–atmosphere model to an increase of atmospheric carbon dioxide. J. Hydrol. 7, 5–23.

Manabe, S., Milly, P.C.D., Wetherland, R., 2004. Simulated long-term changes in river discharge and soil moisture due to global warming. Hydrol. Sci. J. 49, 625–642.

Marshall, L.G., 1985. Geochronology and land-mammal biochronology of the transa-merican faunal interchange. In: Stehli, F., Webb, S. (Eds.), The Great American Biotic Interchange. Plenum Press, New York, pp. 49–88.

Molnar, P., 2008. Closing of the Central American Seaway and the Ice Age: a critical review. Paleoceanography 23. doi:10.1029/2007PA001574 PA2201.

Mosbrugger, V., Utescher, T., Dilcher, D.L., 2005. Cenozoic continental climate evolution of Central Europe. Proc. Natl. Acad. Sci. 102, 14964–14969.

Mudie, P.J., Helgason, J., 1983. Palynological evidence for Miocene climate cooling in eastern Iceland about 9.8 Ma ago. Nature 303, 689–692.

Najjar, R.G., 1999. The water balance of the Susquehanna River basin and its response to climate change. J. Hydrol. 219, 7–19.

Oki, T., 2001. Modeling surface hydrology for global water cycle simulations. In: Matsuno, T., Kida, H. (Eds.), Present and Future of Modelling Global Environmental Change: Toward Integrating Modeling. Terra pub., pp. 391–403.

Owen, J., 1989. Patterns of herpetofaunal species richness: relation to temperature, precipitation, and variance in elevation. J. Biogeogr. 16, 141–150.

Peterson, B.J., Holmes, R.M., McClelland, J.W., Vörösmarty, C.J., Lammers, R.B., Shiklomanov, A.I., Shiklomanov, I.A., Rahmstorf, S., 2002. Increasing river discharge to the Arctic Ocean. Nature 298, 2171–2173.

Poore, H.R., Samworth, R., White, N.J., Jones, S.M., McCave, I.N., 2006. Neogene overflow of Northern Component Water at the Greenland–Scotland Ridge. Geochem. Geophys. Geosyst. 7, Q06010.

Popov, S.V., Ilyina, L.B., Paramonova, N.P., Goncharova, I.A., 2004. Lithological–palaeogeographic maps of Paratethys. Courier Forschungsinstitut Senckenberg 250, 46 p.

Popov, S.V., Shcherba, I.G., Ilyina, L.B., Nevesskaya, L.A., Paramonova, N.P., Khondkarian, S.O., Magyar, I., 2006. Late Miocene to Pliocene palaerogeography of the Paratethys and its relation to the Mediterranean. Palaeogeogr. Palaeoclimatol. Palaeoecol. 238, 91–106.

Prange, M., Schulz, M., 2004. A coastal upwelling seesaw in the Atlantic Ocean as a result of the closure of the Central American Seaway. Geophys. Res. Lett. 31, LI7207.

Rahmstorf, S., 1996. On the freshwater forcing and transport of the Atlantic thermoha-line circulation. Clim. Dyn. 12, 799–811.

Roth, J.M., Droxler, A.W., Kameo, K., 2000. The Caribbean carbonate crash at the middle to late Miocence transition: linkage to the establishment of the modern global ocean conveyor. In: Leckie, R.M., et al. (Ed.), Proceedings of the Ocean Drilling Program. Scientifc Results, 17, pp. 249–273.

Thiede, J., Winkler, A., Wolf-Welling, T., Eldholm, O., Myhre, A.M., Baumann, K.H., Henrichs, R., Stein, R., 1998. Late Cenozoic history of the polar North Atlantic: results from ocean drilling. Quat. Sci. Rev. 17, 185–208.

Tyler, M.J., 1994. Climatic change and its implications for the amphibian fauna. Trans. Royal. Soc. S. Aust. 118, 53–57.

Van Dam, J.A., Alcala, L., Alonso Zarza, A.M., Calvo, J.P., Garces, M., Krijgsman, W., 2001. The Upper Miocene mammal record from the Teruel–Alfambra region (Spain): the MN system and continental Stage/Age concepts discussed. J. Vertebr. Paleontol. 21, 367–385.

Van Dam, J.A., Abdul Aziz, H., Álvarez Sierra, M.A., Hilgen, F.J., Van Den Hoek Ostende, L.W., Lourens, L.J., Mein, P., Van Der Meulen, A.J., Pelaez-Campomanes, P., 2006. Long-period astronomical forcing of mammal turnover. Nature 443, 687–691.

Van Der Meulen, A.J., Pelaez-Campomanes, P., Levin, S.A., 2005. Age structure, residents, and transients of Miocene rodent communities. Am. Nat. 165, 108–125.

Velichko, A.A., Akhlestina, E.F., Borisowa, O.K., Gribchnko, Y.N., Zhidovinov, N.Y., Zelikson, E.N., Iosifova, Y.I., Klimanov, V.A., Morosova, T.D., Nechaev, V.P., Pisareva, V.V., Svetlitskaya, T.V., Spasskaya, I.I., Udartsev, V.P., Faustova, M.A., Shik, S.M., 2005. East European plain. In: Velichko, A.A., Nechaev, V.P. (Eds.), Cenozoic Climatic and Environmental Changes in Russia. Geological Society of America, pp. 31–66.

Westerhold, T., Bickert, T., Röhl, U., 2005. Middle to Late Miocene oxygen isotope stratigraphy of ODP site 1085 (SE Atlantic): new constrains on Miocene climate variability and sea-level fluctuations. Palaeogeogr. Palaeoclimatol. Palaeoecol. 217, 205–222.

Whistler, D.P., Burbank, D.W., 1992. Miocene biostratigraphy and biochronology of the Dove Spring Formation, Mojave Desert, California, and characterization of the Clarendonian mammal age (late Miocene) in California. Geol. Soc. Am. Bull. 104, 644–658.

Winkler, A., Wolf-Welling, T.C.W., Stattegger, K., Thiede, J., 2002. Clay mineral sedimentation in high northern latitude deep-sea basins since the Middle Miocene (ODP Leg 151, NAAG). Int. J. Earth Sci. 91, 133–148.

Wright, J.D., Miller, K.G., 1996. Control of North Atlantic Deep Water circulation by the Greenland–Scotland Ridge. Paleoceanography 11, 157–170.

Zachos, J., Pagani, M., Sloan, L., Thomas, E., Billups, K., 2001. Trends, rhythms, and aberrations in global climate 65 Ma to present. Science 292, 686–693.

Zug, G.R., Vitt, L.J., Caldwell, J.P. (Eds.), 2001. Herpetology. Academic Press, San Diego.